Noise Figure Reduction Techniques in LNA's for Wide Band Multistandard RF Receivers

Giuseppe Martini, Antonio Liscidini and Rinaldo Castello

University of Pavia, Italy

ABSTRACT

LNA's (Low Noise Amplifier) are widely used in wireless portable personal communication systems; the LNA noise directly affects the overall system performances. Here it is shown how the Noise Figure of a RF (Radio Frequency) Receiver can be reduced while satisfying the common constraints of impedance matching at the input, low power consumption and good linearity. The proposed Noise Figure reduction technique is based on the cold resistance approach and negative or positive feedback; a single BJT LNA, derived from the common base configuration, is considered. The Noise Figure reduction is obtained over a wide frequency band of operation, and is thus suitable for Multistandard applications. Different LNA feedback topologies are compared. It is shown that a Noise Figure lower than the limit of the common base configuration can be achieved, along with a current consuption of a few mA, over a wide frequency band of operation. Noise Figure calculations and circuit simulation results are presented and compared.

Keywords: noise figure, low-noise amplifiers, wide band amplifiers, multistandard amplifiers, low-noise LNA, RF amplifiers

1. INTRODUCTION

As consequence of the fast growing and wide spreading of wireless communication, a great number of standards has been developed.[1] These standards, such as GSM, Bluetooth, IEEE 802.11a,b,g, HiperLAN just to mention a few, cover a wide frequency range, roughly between $0.8\,GHz$ and $6\,GHz$.[2,3] The demand for wireless portable personal communication system, capable to interoperate with different standards, and thus different frequencies, requires the development of multiband, multistandard receiver, of which the LNA is a key part. Another key feature of the so called third-generation (3G) receiver is its reconfigurability, needed to adapt the receiver to the various standards, present and future. Starting from these premises, several approaches can be used to implement suitable LNA. One choice is the implementation of individual LNA for each standard,[4] but it has the disadvantage of being area-consuming and poorly configurable. Alternative choices are: narrow band LNA with multiple pass bands,[5] tunable LNA,[6] and wide band LNA.[7] Most promising in 3G applications seem tunable LNA and wide band LNA. In the following we consider two wide band topologies derived from the common base LNA, analyzing their performances in terms of noise figure. Both wide band LNA's can be easily turned into tuned LNA's by simply tuning the load Z_L. An advantage over other topologies is that the load tuning implies the tuning of the input impedance, thus making easy hopping between different frequency bands; input resistance matching is automatically assured for in band signals.

2. LNA NOISE FIGURE

The noise figure F of an LNA, defined, as usual, as the ratio of the output noise power spectrum to the output noise power spectrum due to the source resistance R_s alone, depends mainly on the transconductance g_m of the gain transistor. As a rule of thumb, the greater is g_m, the lower is F. Noise analysis is performet by accounting for white noise sources only, namely, for BJT's, shot noise of the collector bias current I_C and thermal noise of the distributed base resistor r_b,[8] and, for MOSFET's, channel thermal noise with $\gamma = \frac{2}{3}$,[8] thus neglecting any short channel effect.[9] Moreover, for BJT's we assume $\beta = \infty$. The following analysis is performed assuming a wide band load $Z_L = R_L$.

Contact author information: E-mail: martini@unipv.it, Telephone: +39 (0)382 505 784/200,
Web: `http//ele.unipv.it/~ele1/martini`, Address: Department of Electronics, University of Pavia, 1 Via Ferrata, I-27100 Pavia PV, Italy

Noise in Devices and Circuits II, edited by François Danneville, Fabrizio Bonani, M. Jamal Deen, Michael E. Levinshtein Proceedings of SPIE Vol. 5470
(SPIE, Bellingham, WA, 2004) · 0277-786X/04/$15 · doi: 10.1117/12.546958

Downloaded From: http://spiedigitallibrary.org/ on 02/06/2013 Terms of Use: http://spiedl.org/terms

2.1. Common base LNA

In the common base amplifier, which is shown in Fig.1a) for $\zeta = 0$, the input resistance matching condition forces to choose $g_m = \frac{1}{R_s}$, R_s being the source resistance. The voltage gain amounts to $A_v = \frac{V_{out}}{V_s} = \frac{R_L}{2\,R_s}$, and the resulting noise figure is:

$$F = 1 + \frac{r_b}{R_s} + \frac{1}{2}\,\frac{1}{R_s\,g_m} + 4\,\frac{R_s}{R_L} \tag{1}$$

In (1), the second term arises from the thermal noise contribution of the spread base resistance r_b, the third term is due to the shot noise of the bias collector current I_0 of the gain transistor Q, and the fourth term accounts for the thermal noise of the load resistor R_L. The minimum F achievable, for high A_v and negligible base resistance r_b as compared to R_s, amounts to $F_{min} = 1.5\,(1.76\,dB)$. The noise figure and the input resistance cannot be set independently, because the transconductance g_m of Q is the only degree of freedom. In order independently to set up the noise figure from the input resistance, we need one more degree of freedom; the required degree of freedom can be gained by adding some feedback to the common base amplifier. As previously mentioned, F can be lowered by increasing g_m; lowering g_m lowers R_{in}, that has to be recovered to its original value matching R_s. The net result is less noise with the same input resistance; this approach to noise reduction is known as the "cold resistance" approach.[10] One way to recover R_{in} to its initial value is by negative series-shunt feedback[11]; another way is by positive shunt-shunt feedback. Both schemes of feedback are described and discussed in the following.

2.2. Common base LNA with negative series-shunt feedback

The modified common base circuit is shown in Fig.1a). We assume that the transconductance g_m of Q is greater than the amount $\frac{1}{R_s}$ required to satisfy the input resistance matching condition in the common base amplifier.

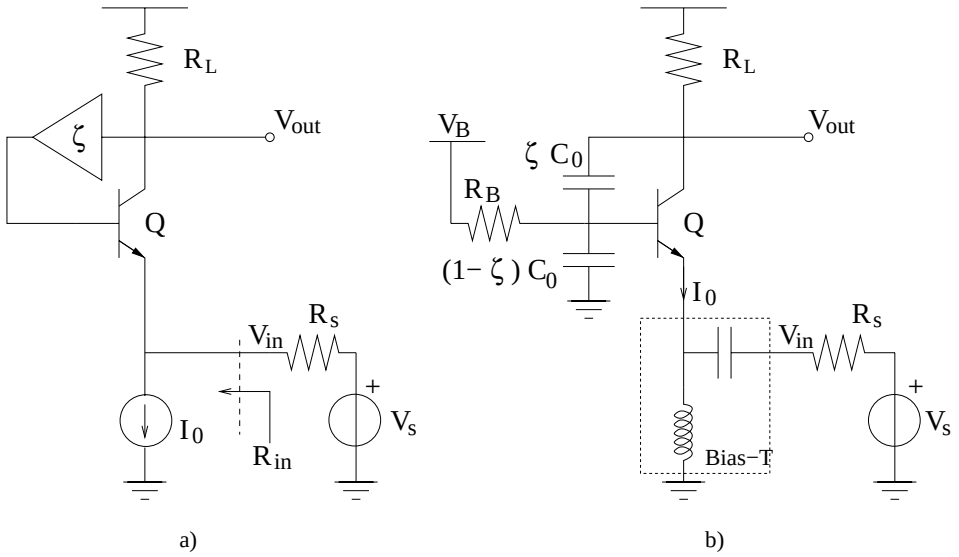

Figure 1. a)Common base LNA with ideal negative series-shunt feedback; it reduces to a common base LNA for $\zeta = 0$. b)Implementation of the LNA in a) with a noiseless capacitive partitioner.

The fraction $\zeta\,V_{out}$ $(0 < \zeta \leq \frac{R_s}{R_L}$, see (3) below) of the output voltage V_{out} is fed to the transistor base, thus reducing the voltage gain $A_v{}' = \frac{V_{out}}{V_{in}}$ and increasing the input resistance R_{in}, both compared to their open loop

Downloaded From: http://spiedigitallibrary.org/ on 02/06/2013 Terms of Use: http://spiedl.org/terms

values. The attenuation ζ can be obtained, in practice, by a capacitive partitioner, that is by a noiseless circuit, as it is shown in Fig.1b). The small signal equivalent circuit used for in band calculation is shown in Fig.2; the voltage generator V_s represents alternatively both the signal source and the thermal noise of the source resistance R_s, depending on what we are calculating. Generators e_b, i_c and e_ℓ are the noise sources arising from r_b, I_C and R_L respectively.

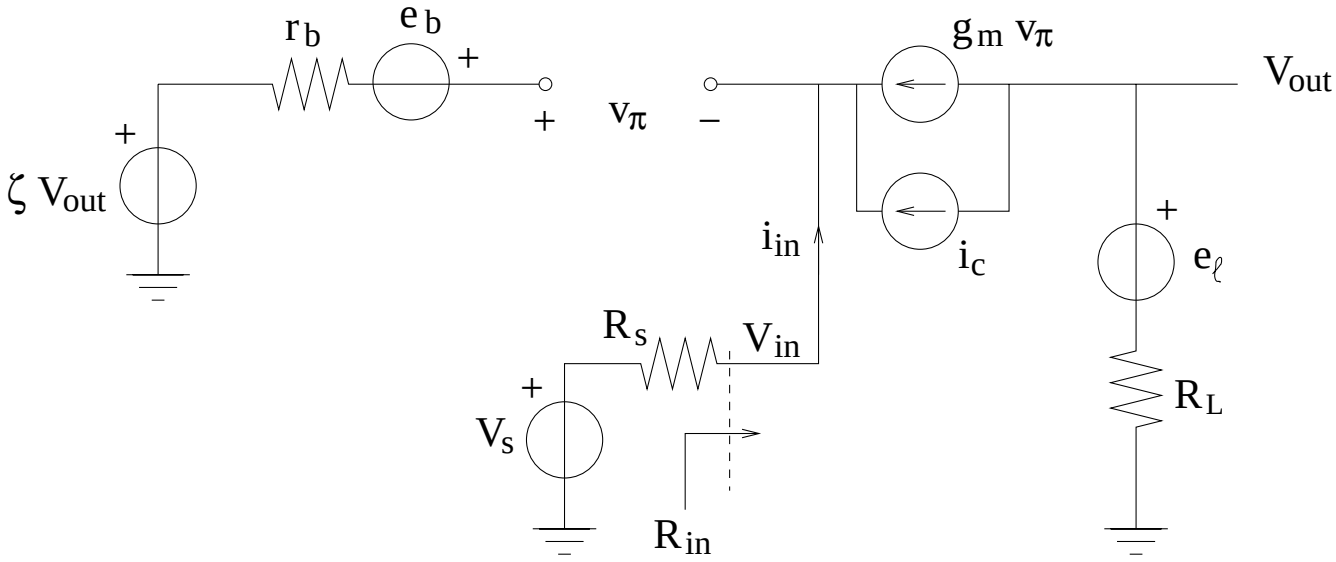

Figure 2. Small signal equivalent circuit of the LNA shown in Fig.1 used for in band calculation.

For given transconductance g_m of Q and feedback amount ζ, the input resistance is given by:

$$R_{in} = \frac{1}{g_m} + \zeta\, R_L \tag{2}$$

and the corresponding feedback amount ζ required to satisfy the input resistance matching condition is:

$$\zeta = \frac{R_s\, g_m - 1}{g_m\, R_L} \tag{3}$$

As a consequence of the input resistance matching condition, the voltage gain $A_v = \dfrac{R_L}{2\, R_s}$ is the same one of the common base amplifier, while the noise figure becomes:

$$F = 1 + \frac{r_b}{R_s} + \frac{1}{2}\,\frac{1}{R_s\, g_m} + \frac{\left(1 + g_m\, R_s\right)^2}{R_L\, R_s\, {g_m}^2} \tag{4}$$

The second term in (4) is the same as in (1) and is unaffected by feedback, because the thermal noise voltage of r_b is seen just as the voltage source signal V_s. The third term in (4) is only formally the same of the corresponding term in (1), the difference from the common base amplifier being that in this case g_m is greater, and consequently the noise contribution from Q is lower. The fourth term in (4) is lower than the corresponding term in (1), again as a consequence of the greater g_m. For negligible r_b and increasing g_m, the minimum achievable noise figure is:

$$F_{min} = 1 + \frac{R_s}{R_L} \tag{5}$$

Downloaded From: http://spiedigitallibrary.org/ on 02/06/2013 Terms of Use: http://spiedl.org/terms

2.3. Common base LNA with positive shunt-shunt feedback

The circuit is shown in Fig.3a). Also in this case we assume that $g_m > \frac{1}{R_s}$. The positive shunt-shunt feedback is provided by the voltage controlled current generator $g_{mM}\, V_{out}$ ($0 < g_{mM} \leq \frac{1}{R_L}$), injecting into the emitter of Q. The effect of the (positive) feedback is an increasing of the transresistance gain $R_m = \frac{V_{out}}{i_{in}}$ and of the input resistance R_{in}, both as compared with their open loop values.

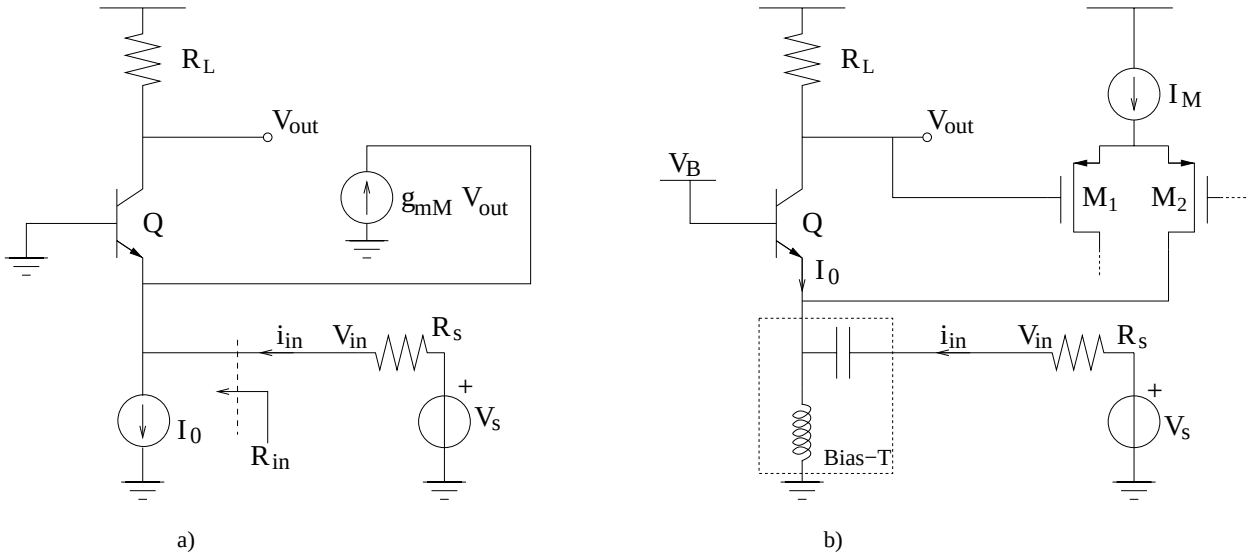

Figure 3. a)Common base LNA with ideal positive shunt-shunt feedback; it reduces to a common base LNA for $g_{mM} = 0$. b)Implementation of the LNA in a) with a MOSFET differential pair in the fedback path; only one half of a fully differential LNA is shown.

A practical implementation of the feedback path can be obtained by a MOSFET differential pair, as it is shown in Fig.3b), where one half of a fully differential LNA is drawn. The small signal equivalent circuit used for calculation is shown in Fig.4. Generators V_s, e_b, i_c and e_ℓ has the same meaning as before; i_M represents the noise introduced by the feedback loop (the differential pair M_1, M_2 in Fig.3b)). For given g_m and feedback amount g_{mM}, the input resistance is:

$$R_{in} = \frac{1}{g_m\,(1 - g_{mM}\,R_L)} \tag{6}$$

The feedback transconductance required to match the input resistance to R_s is:

$$g_{mM} = \frac{g_m\,R_s - 1}{g_m\,R_s\,R_L} \tag{7}$$

In this case, the presence of the positive feedback, along with the input resistance matching condition, gives an increased voltage gain $A_v = \frac{g_m\,R_L}{2} = \frac{R_L}{2\,R_s\,(1 - g_{mM}\,R_L)}$, since the transresitance gain is increased, as compared with its open loop value R_L, up to $\frac{R_L}{(1 - g_{mM}\,R_L)}$, and the input current i_{in} is, because of the input resistance matching condition, always equal to $\frac{V_s}{2\,R_s}$. The noise figure F of this LNA amounts to:

Downloaded From: http://spiedigitallibrary.org/ on 02/06/2013 Terms of Use: http://spiedl.org/terms

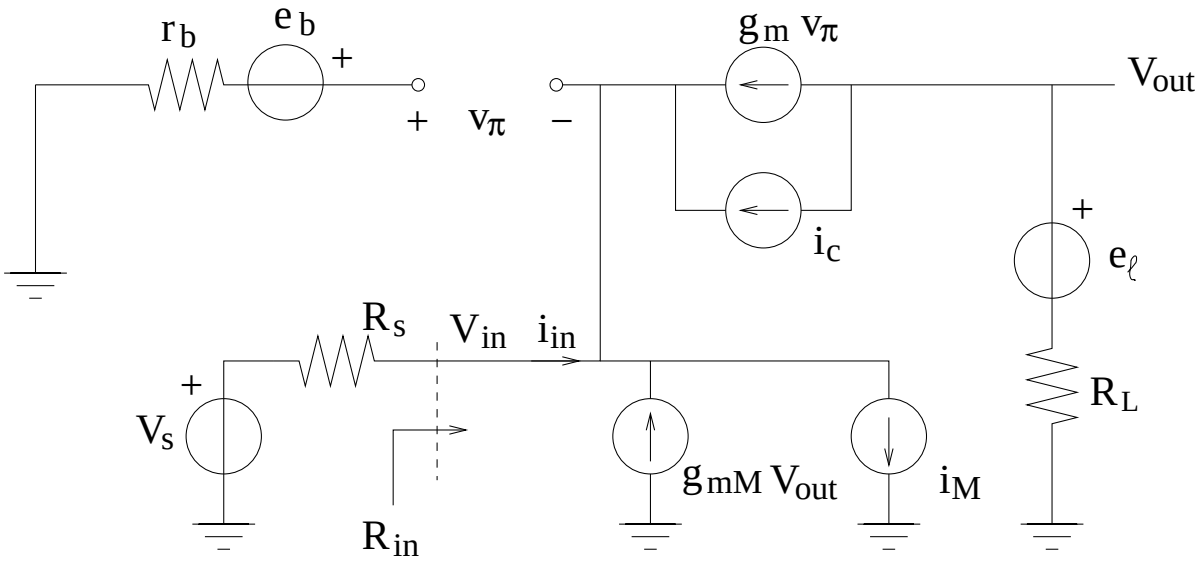

Figure 4. Small signal equivalent circuit of the LNA shown in Fig.3 used for in band calculation.

$$F = 1 + \frac{r_b}{R_s} + \frac{1}{2}\,\frac{1}{g_m\,R_s} + \frac{(1+g_m\,R_s)^2}{R_L\,R_s\,{g_m}^2} + \gamma\,g_{mM}\,R_s \tag{8}$$

and, as compared with (4), one more term, the fifth one, appears in (8); the added term accounts for the noise due to the transconductor M_1, M_2. The minimum noise figure achievable, for negligible r_b and increasing g_m, amounts to:

$$F_{min} = 1 + \frac{R_s}{R_L}\,(1+\gamma) \tag{9}$$

being higher than the correspondig minimum noise figure of the LNA described in Sect.2.2, because of the presence of a noisy transconductor in the feedback loop.

3. CIRCUIT SIMULATION

We perform numerical simulation of the circuits in Fig.1 and Fig.3, in order to verify the accuracy of the calculated noise figures in (4) and (8). We simulate the circuits in Fig.1 and in Fig.3 with $R_s = 50\,\Omega$ and $R_L = 300\,\Omega$, using a BJT with $f_T = 25\,GHz$ and $r_b = 9.3\,\Omega$. The voltage supply is $5\,V$. In all cases the transconductance of Q ranges between $\frac{1}{R_s} = 0.02\,A/V$ and $\frac{5}{R_s} = 0.1\,A/V$.

3.1. Common base LNA with negative series-shunt feedback

Results of simulation of the circuit in Fig.1a) are shown in Fig.5a); all results are plotted vs. the transconductance g_m of Q. Heavy full line is the noise figure F calculated from (4); heavy full line with diamond is the simulated noise figure F. Dotted line, dash dotted line, and dashed line are the contribution to F arising from r_b, collector bias current I_0 and R_L respectively, as calculated from (4); dotted line with circles, dash dotted line with squares, and dashed line with diamonds are the simulated contribution to F arising from r_b, I_0 and R_L respectively. As it can be seen, the agreement between calculated and simulated F and each individual contribution to F is quite good; the difference can be attributed to the series emitter resistance of Q, that is not considered in (4), but it is present in the BJT model used in simulation. The series emitter resistance increases R_{in}, thus causing a mismatch between source resistance and input resistance, and also a reduction of the voltage gain A_v, that, in

Downloaded From: http://spiedigitallibrary.org/ on 02/06/2013 Terms of Use: http://spiedl.org/terms

turn, causes an increasing noise contribution from I_0 and R_L. In Fig.5b) they are shown the results of simulation of the circuit in Fig.1b), with $C_0 = 2\,pF$ and $R_B = 50\,k\Omega$; the circuit in Fig.1b) differs from the one in Fig.1a) because of the non ideal feedback, that is now obtained by a capacitive partitioner. The meaning of the various lines, and lines with symbols, is the same as in Fig.5a). Now the difference between simulated and calculated F is greater than in the previous case of ideal feedback, mainly because of the increased difference between simulated and calculated contribution to F from I_0. The contribution to F from I_0 increases because of the increased mismatch between R_{in} and R_s, due to the presence of the capacitive partitioner in the feedback loop. The trend of calculated and simulated F vs. g_m is the same in both cases. The simulated voltage gain is around 2.8, near to the calculated value of 3, over a band width of the order of $3.5\,GHz$.

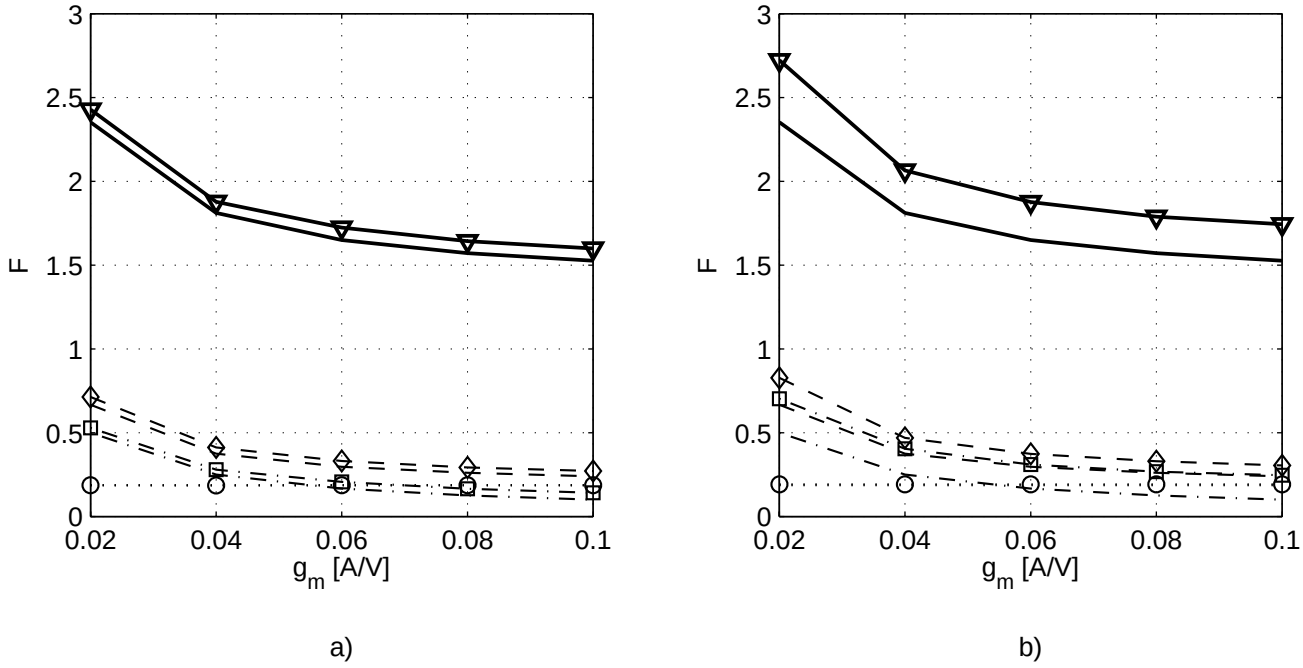

Figure 5. a)Calculated and simulated noise figure of the circuit shown in Fig.1a) (LNA with ideal negative series-shunt feedback). Noise figure F vs. g_m calculated from (4) (heavy full line); contribution to F, calculated from (4), arising from: r_b (dotted line), bias collector current I_0 of Q (dash-dotted line), and R_L (dashed line); simulated F (heavy full line with down triangles); simulated contribution to F arising from: r_b (dotted line with circles), bias collector current I_0 of Q (dash-dotted line with squares), and R_L (dashed line with diamonds). b)Calculated and simulated noise figure of the circuit shown in Fig.1b) (LNA with capacitive negative series-shunt feedback). Noise figure F vs. g_m calculated from (4) (heavy full line); contribution to F, calculated from (4), arising from: r_b (dotted line), bias collector current I_0 of Q (dash-dotted line), and R_L (dashed line); simulated F (heavy full line with down triangles); simulated contribution to F arising from: r_b (dotted line with circles), bias collector current I_0 of Q (dash-dotted line with squares), and R_L (dashed line with diamonds).

3.2. Common base LNA with positive shunt-shunt feedback

In Fig.6a) they are shown the results of simulation of the circuit shown in Fig.3b). Heavy full line is the noise figure F calculated from (8); heavy full line with down triangles is the simulated noise figure F. Dotted line, dash dotted line, dashed line, and light full line are the contribution to F arising from r_b, collector bias current I_0, R_L, and transconductor M_1, M_2 respectively, as calculated from (8); dotted line with circles, dash dotted line with squares, dashed line with diamonds, and light full line with up triangles are the simulated contribution to F arising from r_b, I_0, R_L, and transconductor M_1, M_2 respectively. Also in this case the agreement between calculated and simulated F, and each individual contribution to F, is quite good; once again the difference

Downloaded From: http://spiedigitallibrary.org/ on 02/06/2013 Terms of Use: http://spiedl.org/terms

between simulated and calculated F can be attributed to the series emitter resistance of Q, that is neglected in (8). Very good agreement is observed between calculated and simulated trend of F vs. g_m. The voltage gain depends on g_m, as mentioned in Sect.2.3; the simulated A_v ranges from 3, at $g_m = \frac{1}{R_s}$, up to 12, at $g_m = \frac{5}{R_s}$, while the calculated A_v corresponding to the same range of g_m varies from 3 up to 15. In this case the LNA band width is of the order of $2.5 \div 3.5\,GHz$, depending on the feedback amount.

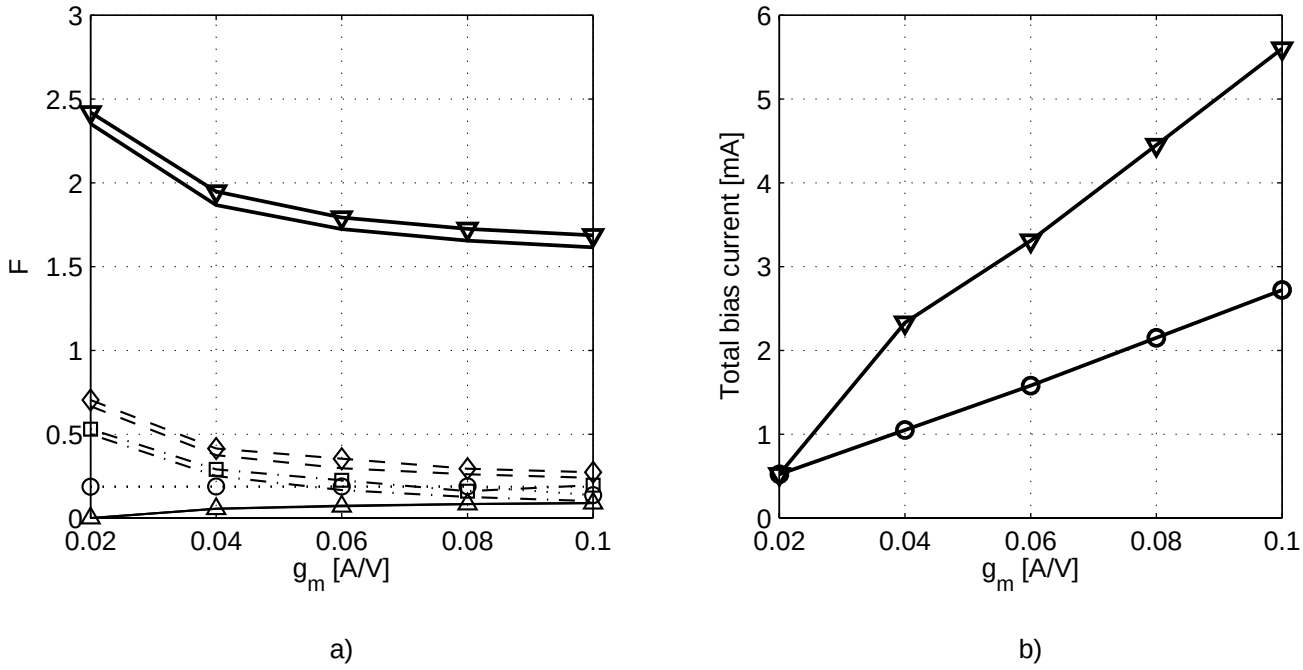

Figure 6. a)Calculated and simulated noise figure of the circuit shown in Fig.3b) (LNA with positive shunt-shunt feedback). Noise figure F vs. g_m calculated from (8) (heavy full line); contribution to F, calculated from (8), arising from: r_b (dotted line), bias collector current I_0 of Q (dash-dotted line), R_L (dashed line), and transconductor M_1,M_2 (light full line); simulated F (heavy full line with down triangles); simulated contribution to F arising from: r_b (dotted line with circles), bias collector current I_0 of Q (dash-dotted line with squares), R_L (dashed line with diamonds), and transconductor M_1,M_2 (light full line with up triangles). b)Total bias current required by the negative series-shunt feedback LNA (full line with down triangles) and by the positive shunt-shunt feedback LNA (full line with circles).

4. COMMENTS AND REMARKS

In this work we analyze the noise behaviour of two LNA topologies, one of them based on a negative series-shunt feedback loop, and the other one based on a positive shunt-shunt feedback loop; both the proposed topologies are derived from the common base amplifier. We show that the noise figure F can be lowered, while maintaining a given input resistance, at the cost of increasing current consumption.

In Fig.6b) it is shown the total bias current required by each of the considered LNA's, vs. g_m. From simulation results, in the negative series-shunt feedback LNA a noise figure F less than 1.7 is achieved at a total bias current of less then $3\,mA$; in the positive shunt-shunt feedback LNA the minimum F obtained from simulation is less than 1.75 at a total bias current of less then $6\,mA$. Such a current consumption is fully compatible with wireless portable personal communication systems. The LNA based on negative feedback achieve a noise figure of about 1.7 with a current consumption of only $3\,mA$, at constant $A_v = 3$; the LNA based on positive feedback loop achieve almost the same low F at roughly twice the current, but with increasing A_v. The positive feedback LNA is thus more tolerant to high noise second stage amplifier or mixer.

Downloaded From: http://spiedigitallibrary.org/ on 02/06/2013 Terms of Use: http://spiedl.org/terms

We conclude that the technique here described permits reduction of the noise figure over a frequency band wide enough to allow the use of the proposed LNA's in wide band, mutistandard portable RF receivers for 3G application.

ACKNOWLEDGMENTS

Giuseppe Martini thanks Vito Svelto for fruitful discussions and constant encouraging. This work was partially funded by "Fondo di Ateneo per la Ricerca" from University of Pavia, and by the national program FIRB from the italian Ministry of Instruction, University and Research (MIUR) under the contract n.RBNE01F582.

REFERENCES

1. H. Elwan, H. Alzaher, and M. Ismail, "A new generation of global wireless compatibility," *IEEE Circuits and Devices Magazine* **17**, pp. 7–19, Jan 2001.
2. S. Andersson, C. Svensson, and O. Drugge, "Wideband lna for multistandard wireless receiver in 0.18 μm cmos," in *Proceedings of the European Solid-State Circuits Conference, ESSCIRC '03*, pp. 655–658, 2003.
3. S. Mou, J. Ma, K. S. Yeo, and M. A. Do, "A cmos rf bandpass low noise amplifier for multi-band wireless communication applications," in *Proceedings of IEEE Radio and Wireless Conference RAWCON 2002*, pp. 225–228, 11-14 Aug 2002.
4. A. Savla, A. Ravindran, J. Leonard, and M. Ismail, "System analysis of a multi-standard direct conversion wireless receiver," in *Circuits and Systems, The 2002 45th Midwest Symposium on, MWSCAS-2002.*, **3**, pp. III–401–III–404, 4-7 Aug 2002.
5. H. Hashemi and A. Hajimiri, "Concurrent multiband low-noise amplifiers-theory, design, and applications," *IEEE Trans. Microwave Theory Tech.* **50**, pp. 288–301, 2002.
6. M. Benmansour and P. Mukund, "A tuned wideband lna in 0.25 /spl mu/m ibm process for rf communication applications," in *VLSI Design, Proceedings of the 17th International Conference on,*, pp. 631–634, 5-9 Jan 2004.
7. Adiseno, H. Magnusson, and H. Olsson, "A 1.8-v wide-band cmos lna for multiband multistandard front-end receiver," *Proceedings of the European Solid-State Circuits Conference, ESSCIRC '03* , pp. 141–144, 2003.
8. A. van der Ziel, *Noise in Solid State Devices and Circuits*, John Wiley and Sons, Inc., New York, 1986.
9. A. Scholten, H. Tromp, L. Tiemeijer, R. V. Langevelde, R. Havens, P. D. Vreede, R. Roes, P. Woerlee, A. Montree, and D. Klaassen, "Accurate thermal noise model for deep-submicron cmos," in *Technical Digest of IEDM , International Electron Devices Meeting*, pp. 155–158, 1999.
10. R. Chase, C. de La Taille, S. Rescia, and N. Seguin, "Transmission line connections between detector and front end electronics in liquid argon calorimetry," *Nucl. Instrum. & Meth.* **A330**, pp. 228–242, 1993.
11. A. Sedra and K. Smith, *Microelectronic Circuits*, Fourth Edition, Oxford University Press, New York, 1998.

Downloaded From: http://spiedigitallibrary.org/ on 02/06/2013 Terms of Use: http://spiedl.org/terms